



Power Electronic Systems  
Laboratory

© 2018 Springer

Springer Nature, Electrical Engineering, Vol. 100, No. 3, pp. 2085-2094, September 2018

## **Unified Power Flow Analysis of String Current Diverters**

M. Kasper,  
D. Bortis,  
J. W. Kolar

This is a post-peer-review, pre-copyedit version of an article published in Electrical Engineering. The final authenticated version is available online at: <https://doi.org/10.1007/s00202-018-0682-z>



Eidgenössische Technische Hochschule Zürich  
Swiss Federal Institute of Technology Zurich

# Unified Power Flow Analysis of String Current Diverters

Matthias Kasper · Dominik Bortis · Johann W. Kolar

Received: 21 July 2017 / Accepted: 19 February 2018

**Abstract** In this paper, a unified power flow analysis is proposed for current diverters which are used for balancing series stacked voltage domains, e.g. employed in photovoltaic (PV) energy systems or auxiliary power supplies with very high DC input voltage. This analysis allows to easily derive the power levels processed by the current diverters for any given operating point of the attached sources and/or loads representing the voltage domains. The proposed analysis is applied to two examples; on the one hand PV systems are investigated where it is revealed, that power limited current diverters can only offer a benefit for light shading scenarios, and on the other hand auxiliary power supplies with extremely high voltage conversion ratios are investigated.

**Keywords** Current Diverters · Voltage Balancing · Partial Power Converters

## 1 Introduction

Partial power processing converter architectures [1] for balancing series connected sources and/or loads, i.e. in general a string of voltage domains or cells, have gained significant interest in the past, due to their capability of balancing local asymmetries in voltages by processing only a fraction of the full system power. This enables high conversion efficiencies and small converter volumes compared to full-power converters, since the converter

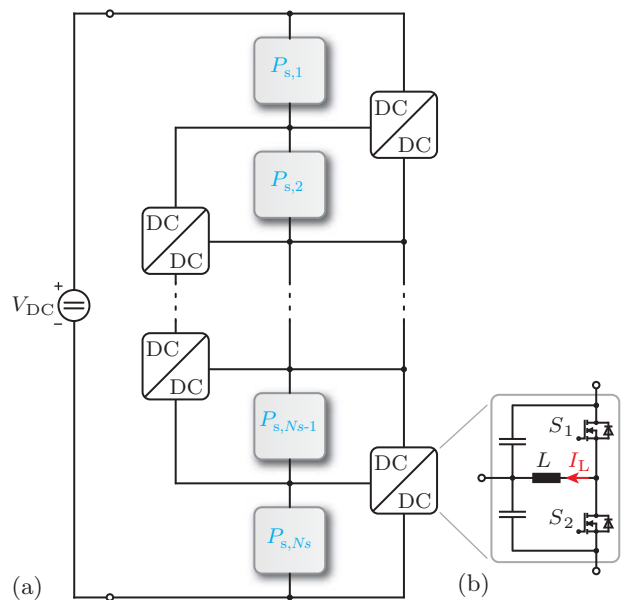


**Fig. 1** Generalized application of string current diverters consisting of  $N_s$  series stacked cells and  $N_b = N_s - 1$  current diverter modules. Each cell can either be a power source, power sink, or storage element without any net power flow. Therefore, considering stationary operation, the values  $P_{s,i}$  can either be positive (i.e. loads), negative (i.e. generators) or zero (i.e. capacitors). (b) Possible implementation of a current diverter module as inverting buck-boost DC/DC converter.

modules can have a low power rating and their efficiency has a reduced impact on the total conversion efficiency. Popular applications for a DC current diverter concept are battery state-of-charge (SOC) equalization [2, 3], data center power distribution [4], multistage stacked boost converters [5–7], stacked voltage domains for CPU power delivery [8], photovoltaic (PV) energy systems [9–13] and auxiliary supplies for extremely high conversion ratios [14]. The common struc-

M. Kasper (kasper@lem.ee.ethz.ch)  
D. Bortis (bortis@lem.ee.ethz.ch)  
J. W. Kolar (kolar@lem.ee.ethz.ch)

Power Electronic Systems Laboratory  
ETH Zurich  
Physikstrasse 3  
8092 Zurich, Switzerland

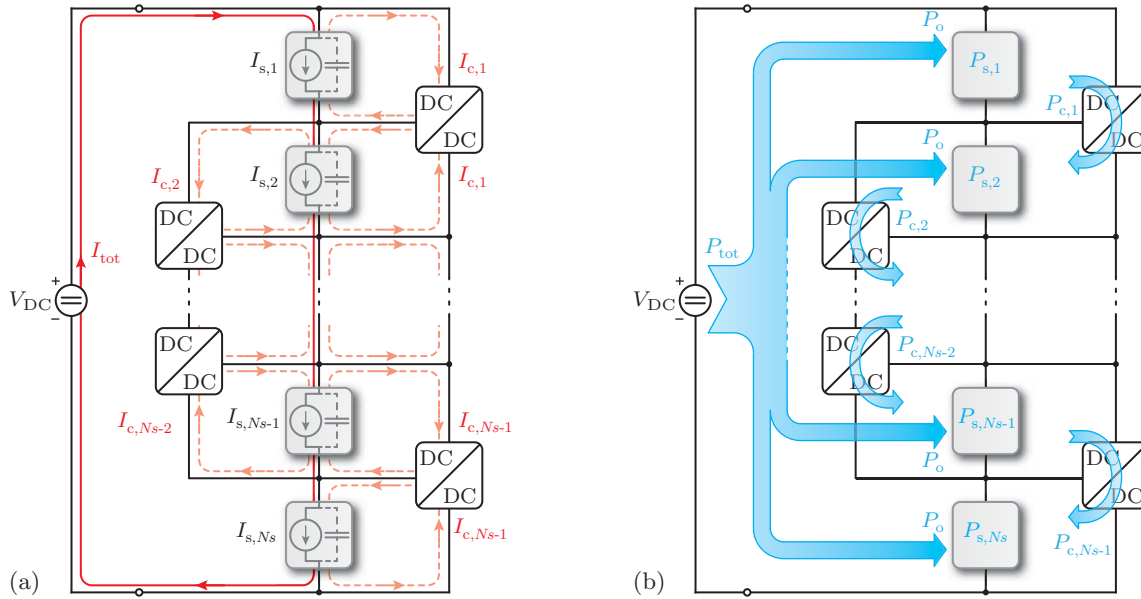


**Fig. 2** Detailed steady-state analysis of (a) the current flow, and (b) the power flow in the generalized current diverter system balancing a string of cells. In (a) the cells are modeled as current sources  $I_{s,i}$ . The current  $I_{tot}$  from the DC-link flows through all current sources while the difference between  $I_{tot}$  and the currents of the individual sources is compensated by the diverter modules with currents  $I_{c,i}$ . Since the voltages of all cells are equalized, the power flow analysis of (b) can be based on the derived currents, which shows that finally each cell receives the power  $P_0$  from the DC-link (or delivers it to the DC-link, depending on the sign of  $P_0$ ). Accordingly, the current diverters are compensating the mismatch between the individual cell power levels  $P_{s,i}$  and  $P_0$ .

ture of these systems is a series stack (string) of multiple cells, acting as power sources or loads, where around every two neighboring cells a string current diverter module is connected (cf. **Fig. 1(a)**). The basic implementation of the current diverters is with inverting buck-boost converters operated with a fixed duty cycle of  $D = 0.5$  in order to equally balance the voltages between adjacent cells for stationary operation.

Even though the current diverters have been in the focus of research for many years, there are still no general design guidelines for the diverter modules. Especially in the area of PV energy systems, the design of the diverters is strongly dependent on the number of PV modules in a string and the expected worst case shading scenario (cf. [15, 16]). Accordingly, in this paper a universal power flow analysis is introduced, which allows to easily identify the power level which is processed by any diverter module for a given scenario of stacked voltage sources and/or loads, irrespective of the underlying application. Based on the analysis presented in **Sec. 2**, the required specifications for the design of the diverter modules can be derived, which is demonstrated for a PV system application in **Sec. 3**. In addition, the impact of limited power ratings of the diverter modules on the power output of the PV string is investigated. In **Sec. 4**, the proposed method is applied to auxiliary power supplies with high step-down conversion ratios,

termed “Rainstick” converters. Finally, the concept of coupling the inductors of the diverter modules and the associated advantages and disadvantages are analyzed in **Sec. 5**.

## 2 Power Flow Analysis

From a general point of view, the structure of any system with current diverters consists of  $N_s$  cells acting as sources/sinks and  $N_b = N_s - 1$  diverter modules, as shown in **Fig. 2(a)**. In steady state operation, the stacked cells can be modeled as current sources/sinks  $I_{s,1} \dots I_{s,N_s}$  and a capacitive storage element connected in parallel, as indicated by the grey blocks in **Fig. 2(a)**.

Depending on the type of operation and/or application, the current sources/sinks can have one of the following three states (sign of  $I_{s,i}$  with  $i \in \{1, N_s\}$ ):

- *Positive*: Operation as a sink, i.e. load;
- *Negative*: Operation as a source, e.g. PV module;
- *Zero*: No net power flow, i.e. capacitor (storage).

Based on Kirchhoff’s current law the currents of series connected cells have to be equal (in case no current diverters are employed). Depending on the application, however, the current values of the individual cells might be different, e.g. due to different light irradiation on the PV modules in a string. Therefore, current diverters have to be added around adjacent cells in

order to decouple the operation of the individual cells and to allow an operation of each cell in the maximum power point. In this case, the current diverter modules conduct the currents  $I_{c,i}$  which is the difference between the total current  $I_{\text{tot}}$  flowing from the DC-link through the series stacked cells and the cell currents  $I_{s,i}$  (cf. **Fig. 2(a)**). Based on that, for each node the current balance equation can be stated, e.g. for the first node  $I_{\text{tot}} - I_{s,1} - I_{c,1} = 0$ , and for the second node  $I_{s,1} - I_{s,2} + 2I_{c,1} - I_{c,2} = 0$ , etc.. These equations can be reformulated as

$$I_{s,i} = I_{\text{tot}} + I_{c,i-1} - I_{c,i} \quad (1)$$

with  $i \in \{1, N_s\}$ .

Based on this set of equations, the total current  $I_{\text{tot}}$  can be derived as the average current of all cells, i.e.

$$I_{\text{tot}} = \frac{\sum_{i=1}^{N_s} I_{s,i}}{N_s}. \quad (2)$$

In addition, the currents conducted by the individual current diverters can be determined as

$$I_{c,i} = \frac{1}{N_s} \left( i \cdot \underbrace{\sum_{j=i+1}^{N_s} I_{s,j}}_{\textcircled{1}} - (N_s - i) \cdot \underbrace{\sum_{j=1}^i I_{s,j}}_{\textcircled{2}} \right). \quad (3)$$

It can be seen, that the current conducted by any current diverter module is influenced by all cells, since the current level is calculated by weighting the sum  $\textcircled{1}$  of all cell currents “below” the diverter module with the number  $i$ , which is the number of cells “above” this diverter, and subtracting the sum  $\textcircled{2}$  of the cell currents “above” the diverter module weighted with the number of cells  $N_s - i$  “below”. For the case that all cells have equal current values (i.e.  $I_{s,1} = I_{s,2} = \dots = I_{s,N_s}$ ), the current levels in all diverter modules become zero, which is in accordance with the expectation that no current transfer through the diverter modules is necessary in case of missing mismatch and/or perfect balance.

As a result of the employment of current diverters, the voltages of all series stacked cells are equalized to  $V_{s,i} = V_{\text{DC}}/N_s$ . In combination with the previously derived current equations, the system operation can also be described with respect to the power flow (cf. **Fig. 2(b)**). Each cell can thus be regarded as a power source/sink with one of the following three states (sign of  $P_{s,i}$  with  $i \in \{1, N_s\}$ ):

- *Positive*: Operation as a power sink, i.e. load;
- *Negative*: Operation as a power source, e.g. PV module;
- *Zero*: No net power flow, i.e. capacitor (storage),

which can be written in a vector form as

$$\vec{p}_s = (P_{s,1}, P_{s,2}, \dots, P_{s,N_s}) \quad (4)$$

to simplify the notation. The total current  $I_{\text{tot}}$  which flows through all cells can be regarded as the total power  $P_{\text{tot}}$  which is directly transferred from the DC-link  $V_{\text{DC}}$  to the individual cells, or vice versa. This means, that each cell provides/receives the power  $P_o$  directly to/from the DC-link source  $V_{\text{DC}}$ , which is the average value of the power levels of all power sources, i.e.

$$P_o = \frac{\sum_{i=1}^{N_s} P_{s,i}}{N_s} = \frac{P_{\text{tot}}}{N_s}. \quad (5)$$

Thus, the current diverters only balance the power asymmetries among the stacked power sources such that the difference between the average power  $P_o$  and the actual power level  $P_{s,i}$  of a power source is compensated. By taking into account, that, based on (1), for each of the stacked cells a power balance has to prevail (i.e.  $-P_{s,i} + P_o + P_{c,i-1} - P_{c,i} = 0$  for a cell with index number  $i$ ), the set of equations for all cells can be solved to find the levels of power which are transferred by the current diverter modules, i.e.  $\vec{p}_c = (P_{c,1}, P_{c,2}, \dots, P_{c,N_s-1})$ , as

$$P_{c,i} = \frac{1}{N_s} \left( i \cdot \sum_{j=i+1}^{N_s} P_{s,j} - (N_s - i) \cdot \sum_{j=1}^i P_{s,j} \right), \quad (6)$$

which is in analogy with (3), if both sides of (3) are multiplied with  $V_{s,i} = V_{\text{DC}}/N_s$ .

### 3 PV Energy Systems

In order to mitigate the effects of mismatched operation conditions in a PV system, current diverter modules (also termed parallel-connected partial-power module integrated converters [17], or power shufflers) can be installed to operate all PV modules close to their maximum power points (MPPs) [18], as shown in **Fig. 3**. Thus, the vector of power sources  $\vec{p}_s$  can be written as

$$\vec{p}_s = (-P_{\text{MPP},1}, -P_{\text{MPP},2}, \dots, -P_{\text{MPP},N_{\text{PV}}}), \quad (7)$$

$P_{\text{MPP},i} > 0$ , for a system with  $N_{\text{PV}}$  PV modules.

In the following, a worst case scenario is considered, where the string of PV modules is divided into a shaded part and an unshaded part. It is assumed that the first  $n$  PV modules are shaded and have a maximum power generation of  $k_{\text{sh}} \cdot P_{\text{MPP}}$  per PV module, and the remaining  $N_{\text{PV}} - n$  PV modules are unshaded with a maximum output power of  $P_{\text{MPP}}$ . According to (5), the

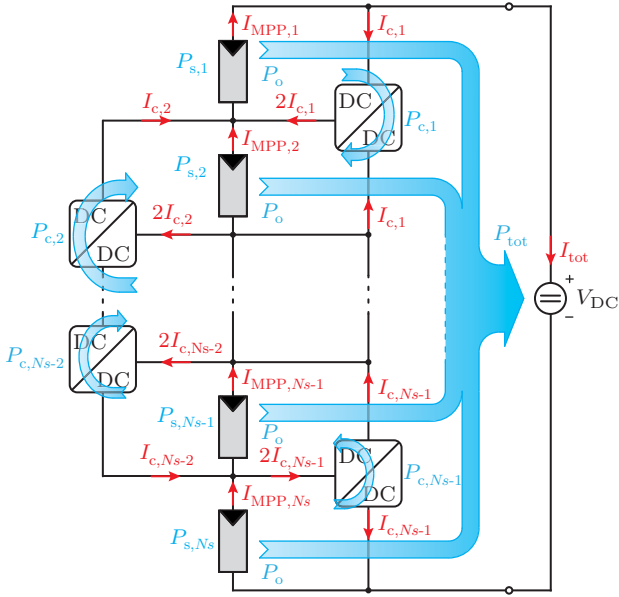


**Fig. 3** Analysis of the current and power flow in a PV system with current diverter modules. The PV modules are replaced with current sources, and the cell currents have negative values ( $I_{s,i} = -I_{MPP,i}$ ) and also the total current  $I_{tot}$  has a negative value, according to (2), and thus flows into the DC-link. Therefore, the physical direction of the power flow is from the PV modules to the DC-link. The power which is processed by the individual diverter modules depends on the actual shading scenario and is not equal for all diverter modules.

average power which is directly transferred from each PV modules to the DC-link source is

$$P_o = -\frac{n \cdot k_{sh} \cdot P_{MPP} + (N_{PV} - n) \cdot P_{MPP}}{N_{PV}}. \quad (8)$$

Regarding the diverter modules in this scenario, the amount of power which has to be processed in each diverter module  $n$  can be calculated as

$$P_{c,n} = -\frac{P_{MPP}}{N_{PV}} \cdot (n \cdot (N_{PV} - n) - n \cdot (N_{PV} - n) \cdot k_{sh}). \quad (9)$$

In case half of the PV string is shaded and the other half is unshaded, the maximum of (9) can be found at  $n = \frac{N_{PV}}{2}$ , which means that the diverter module at the boarder of the shaded and unshaded section of the PV string has to process the largest amount of power. The power flow through the balancing converter connecting the two sections is then

$$|P_{c,max}| = \frac{N_{PV}}{4} \cdot P_{MPP} \cdot (1 - k_{sh}). \quad (10)$$

As can be seen clearly in (10),  $P_{c,max}$  is not only proportional to the PV modules power  $P_{MPP}$  and  $k_{sh}$  but also to the total number  $N_{PV}$  of PV modules in

the string. Thus, by relating the maximum converter power to the MPP power of the unshaded PV modules, i.e.  $r_p = |P_{c,max}|/P_{MPP}$ , the number of PV modules in the string can be found, where a certain power ratio  $r_p$  is reached that depends on the light transmissibility factor of the shade,  $k_{sh}$ , as

$$N_{PV} = \frac{4 \cdot r_p}{1 - k_{sh}}. \quad (11)$$

As an example of this worst case scenario, for a string with  $N_{PV} = 20$  PV modules out of which the first (or last) 10 PV modules are shaded, assuming  $k_{sh} = 0.8$  (i.e. the shaded PV modules deliver 80% of the power of the unshaded PV modules output power  $P_{MPP}$ ) the diverter module in between the shaded and the unshaded section of the string has to already process 100% of the power of an unshaded PV module ( $P_{MPP}$ ), i.e.  $r_p = 1$ . Hence, this diverter module would have to be designed for the same power rating as a power converter processing the full power of a PV module [17] and would thus nullify the advantages of the partial power conversion. For even more severe shading scenarios (i.e. lower  $k_{sh}$ ) the situation becomes even worse and the most affected current diverter module has to process a multiple of the power of a single PV module.

### 3.1 Implications of Power Limitations

This dependency of the required power rating of the current diverter on the shading scenario and the string length complicates the converter design. As a natural consequence, the power rating of the current diverters has to be limited to a defined value, which, however, will no longer allow to operate all PV modules in their respective MPPs at all times, as explained below.

Considering again the same worst case scenario where a string with  $N_{PV}$  PV modules is equally split into a shaded and an unshaded section, the total theoretically available power of the entire string is

$$P_{th,max} = \frac{N_{PV}}{2} \cdot P_{MPP} \cdot (1 + k_{sh}). \quad (12)$$

which is shown in **Fig. 4** (normalized to  $P_{max} = N_{PV} \cdot P_{MPP}$ ) as the topmost line with the highest power.

In state-of-the-art systems with only bypass diodes, the string can either be operated at the MPP current level of the unshaded PV modules, i.e. bypassing the shaded PV modules, which yields an output power of  $P_{D2} = N_{PV}/2 \cdot P_{MPP}$  (horizontal line at 0.5 in **Fig. 4**), or all PV modules can be operated at the MPP current level of the shaded PV module, which results in an output power of  $P_{D1} = N_{PV}/2 \cdot k_{sh} \cdot P_{MPP}$  (diagonal line in **Fig. 4** from  $(k_{sh}, P/P_{max}) = (1, 1)$  to  $(0, 0)$ ).

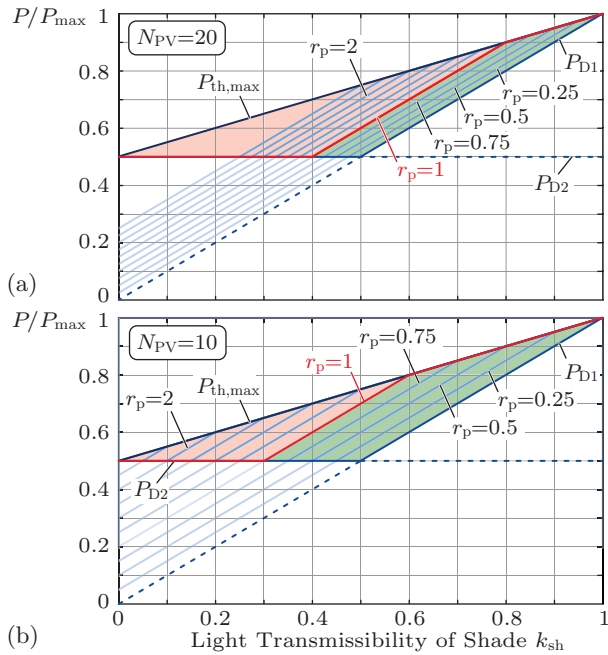


**Fig. 4** Influence of the current diverter power rating  $r_p$  on the harvested power of a string with  $N_{PV}$  PV modules for different shading intensities for the worst case scenario (half of the PV is string unshaded and the other half is shaded). The red colored area defines the power which cannot be harvested even when the diverter modules are sized for the full power of an unshaded PV module, i.e. for  $r_p = 1$ . Hence, the benefit provided by current diverters, visualized by the green colored area, is small.

In the case where current diverters with a limited power rating of  $r_p = |P_{c,max}|/P_{MPP}$  are used, the maximum theoretically available string power  $P_{th,max}$  can only be harvested above a light transmissibility factor  $k_{sh}$  of the shade of

$$k_{sh} \geq 1 - \frac{4 \cdot r_p}{N_{PV}} \quad (13)$$

which can be derived from (11). If the light transmissibility falls below this limit, the only way to keep the power of the current diverters at or below their maximum power rating is to operate the unshaded PV modules at an operating point  $P_{PV,sub} = k_{PV,lim} \cdot P_{MPP}$  below their MPP. The factor of power reduction  $k_{PV,lim}$  can be derived by modifying (10) to be

$$|P_{c,max}| = N_{PV}/4 \cdot P_{MPP} \cdot (k_{PV,lim} - k_{sh}). \quad (14)$$

Inserting the relationship of  $|P_{c,max}| = r_p \cdot P_{MPP}$  and solving the equation for  $k_{PV,lim}$  yields  $k_{PV,lim} = k_{sh} + 4 \cdot r_p/N_{PV}$ . Based on this, the total power that can be harvested from a string of PV modules under the worst case shading scenario (i.e. splitting the string into two equal sections), can be derived for power limited current diverters as

$$P_{out,lim} = \frac{N_{PV}}{2} \cdot P_{MPP} \cdot \left( 2 \cdot k_{sh} + \frac{4 \cdot r_p}{N_{PV}} \right) \quad (15)$$

(blue parallel lines in **Fig. 4**) which are valid for  $k_{sh} \leq 1 - 4 \cdot r_p/N_{PV}$ . For  $k_{sh} \geq 1 - 4 \cdot r_p/N_{PV}$ , the total available power  $P_{th,max}$  can be harvested. In addition, when  $P_{out,lim}$  drops below  $P_{D2}$  the operation of the current diverters no longer provides any benefit. In this case, the shaded PV modules are advantageously bypassed by the bypass diodes and the unshaded PV modules are operated at their respective MPPs. Hence, in contrast to a first guess, the useful operating range and the benefit of current diverters are rather limited, as the two following examples show.

The results of the calculations above are visualized for string lengths of  $N_{PV} = 20$  and  $N_{PV} = 10$  in **Fig. 4(a)** and **(b)**, respectively. It can be seen, that even if the current diverters are designed for the full power rating of an unshaded PV module (i.e.  $r_p = 1$ , which is what full-power converter concepts require [17]), it is not possible to harvest all of the string power  $P_{th,max}$  for shading factors below  $k_{sh} \leq 0.8$  or  $k_{sh} \leq 0.6$ , respectively, (red colored area represents the lost power for  $r_p = 1$ ). The green colored area depicts the extension of the operating range concerning the additional power which can be harvested in case the current diverters are employed (for  $r_p = 1$ ) in comparison to low-cost state-of-the-art solutions with simple bypass diodes, which is +20% of  $P_{max}$  for the case of  $N_{PV} = 10$  and only +10% of  $P_{max}$  for  $N_{PV} = 20$ . Please note, that this consideration does not include any losses of the current diverters, which will further decrease the benefits of employing current diverters.

### 3.2 Efficiency Considerations

For an efficiency comparison of the string current diverter concept with a traditional series connected full-power converter concept (typically consisting of buck-boost converters [17]), the worst case shading scenario is considered again, where the PV string is divided into a shaded and an unshaded half. The efficiency of either one of the concepts can be calculated as

$$\eta = \frac{P_{out}}{P_{in}} = \frac{\sum_{i=1}^{N_{PV}} P_{PV,i} - \sum_{i=1}^{N_c} P_{Loss,i}}{\sum_{i=1}^{N_{PV}} P_{MPP,i}} \quad (16)$$

which depends on the converter losses  $P_{Loss,i}$ , the generated power of the PV panels  $P_{PV,i}$ , and the theoretically available power of the panels  $P_{MPP,i}$ . For a fair comparison, it is assumed that the converters for both concepts are designed for the same maximum power

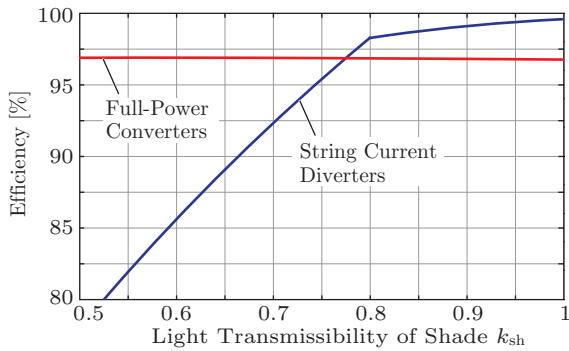


**Fig. 5** Comparison of the efficiency of a string with  $N_{PV} = 20$  PV panels equipped either with series connected full-power converters or with string current diverters with the same power rating. One half of the PV string is unshaded and generates  $P_{MPP} = 250$  W per panel, while the other half is shaded where each panels produces  $P_{PV} = k_{sh}P_{MPP}$ . The converters of both concepts have the same efficiency characteristic.

rating  $P_{c,max} = P_{MPP}$  (i.e.  $r_p = 1$ ), and that they exhibit the same efficiency characteristic in dependency of the processed power. This means, they have the loss characteristic,

$$P_{Loss}(P) = a + b \cdot P + c \cdot P^2, \quad (17)$$

composed of a constant term ( $a$ , i.e. control losses), a term proportional to the processed power ( $b \cdot P$ , i.e. diode conduction losses), and a term proportional to the square of the processed power ( $c \cdot P^2$ , i.e. resistive losses). For a PV string with  $N_{PV} = 20$  PV panels, an MPP power of  $P_{MPP} = 250$  W and an assumed efficiency characteristic ( $a = 1$ ,  $b = 0.0125$ ,  $c = 0.0000625$ ), the efficiency of both concepts can be calculated for different values of  $k_{sh}$  for the worst case shading scenario, as shown in **Fig. 5**. It can be noticed, that the efficiency of the string current diverters is greater than the efficiency of the full-power converters for high values of  $k_{sh}$ , i.e. similar power levels of the shaded and unshaded panels. Below  $k_{sh} = 0.8$ , the string current diverter placed at the border between the shaded and unshaded section of panels reaches its maximum power limit and forces the unshaded panels to operate below their MPP, i.e.  $P_{PV,i} \neq P_{MPP,i}$  (cf. **Fig. 4(a)**). This reduces the efficiency of the system, since power is lost that could have been harvested. In contrast, the full-power concept shows a very flat efficiency curve with little dependency on  $k_{sh}$  because the PV panels can be operated in the MPP for all values of  $k_{sh}$ .

One possibility to reduce the probability of the worst case shading scenario could be to wire the PV panels in a different pattern, such that PV panels from different locations on the roof are connected to each other. As a result, the PV string would not be divided into

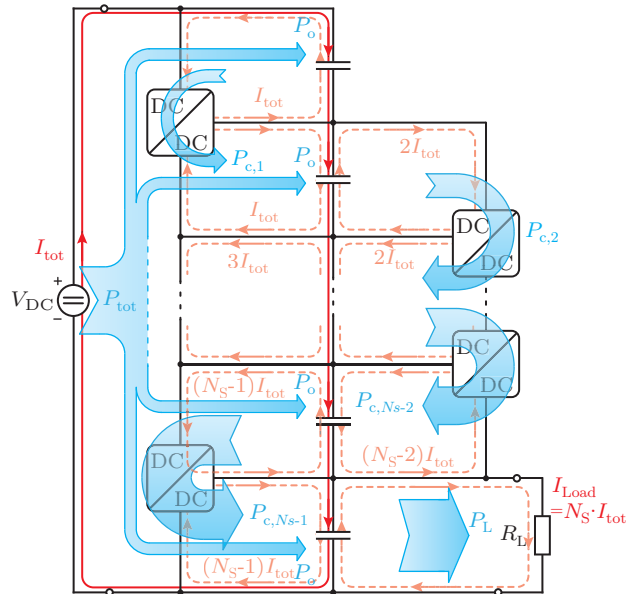


**Fig. 6** Analysis of a cellular converter with high conversion ratio consisting of series stacked capacitors and current diverter modules. The power  $P_0$  is directly delivered from the source to the load, while the rest (i.e.  $(N_s - 1) \cdot P_o$ ) is shuffled through the diverter stages.

a shaded and unshaded part, but would have shaded and unshaded panels connected in an alternating fashion. However, this would come at the expense of greater wiring efforts and conduction losses.

#### 4 High Step-Down Conversion Ratio “Rainstick” DC/DC Converters

Another application for current diverter modules are (auxiliary) power supplies with high conversion ratios [14]. In this application, the current diverter modules are connected around a stack of series connected capacitors, where e.g. a supplying voltage source  $V_{DC}$  is connected in parallel to the stack of capacitors and the load  $R_L$  is attached to the bottom capacitor, as depicted in **Fig. 6**. The blocking voltage stress on the current diverter power transistors is defined by the capacitor voltages and ideally, i.e. for perfect balance, amounts to only a fraction  $V_{DC}/N_s$  of the total input voltage  $V_{DC}$ . Therefore, assuming a certain power transistor blocking capability, the achievable conversion ratio is determined by the number  $N_s$  of employed capacitors. According to the definitions of **Sec. 2**, the vector of power sources becomes  $\vec{p}_s = (0, 0, \dots, 0, P_L)$  in this case. Consequently, the power  $P_0$  which is directly delivered from the source to the load (i.e. flowing through the series connected ca-

pacitors) is

$$P_o = \frac{P_L}{N_s}. \quad (18)$$

The remaining part of the load power (i.e.  $(N_s - 1) \cdot P_o$ ) has to be delivered by the diverters. The power level which is processed by each current diverter module depends on the position of the diverter in the stack and can be determined with (6) as

$$\begin{aligned} P_{c,i} &= \frac{1}{N_s} \left( \underbrace{i \cdot \sum_{j=i+1}^{N_s} \vec{p}_s(j)}_{=P_L \cdot i} - \underbrace{(N_s - i) \cdot \sum_{j=1}^i \vec{p}_s(j)}_{=0} \right) \\ &= \frac{P_L \cdot i}{N_s}. \end{aligned} \quad (19)$$

This means, that the largest amount of power is processed by the converter closest to the load, i.e.  $i = N_s - 1$  which yields

$$P_{c,\max} = P_L \cdot \frac{(N_s - 1)}{N_s} \quad (20)$$

and approaches the load power  $P_{c,\max} \approx P_L$  for high numbers of  $N_s$ . As a result, for large conversion ratios the current diverters have to be designed for almost the same power rating as the load power, reducing the benefits of the partial power conversion concept. Furthermore, the total system efficiency contains a multiplication of the efficiencies of the individual diverter modules [14], which strongly limits the achievable total conversion efficiency for systems with a high number of diverter modules. However, as mentioned above, the modular structure of the system facilitates a design of the diverter modules for only a fraction of the entire DC-link voltage, which enables the use of semiconductors with reduced blocking voltage compared to full-power concepts. In addition, the modular structure allows for an easy realization of the system by employing multiple diverters modules with identical hardware and the extension to different input voltage levels with a different number of modules (scalability), potentially offering cost benefits. Another advantage is the simple and robust control of each diverter module with fixed duty cycles of 50% without any communication between the diverters. Thus, this conversion concept is especially well suited for high-voltage and high-power environments (e.g. traction applications) where low-voltage equipment with a low power rating has to be supplied and a high conversion ratio is required (e.g. as an auxiliary supply). For this type of application, the limited conversion efficiency of this supply is of minor concern and will not affect the efficiency of the overall system

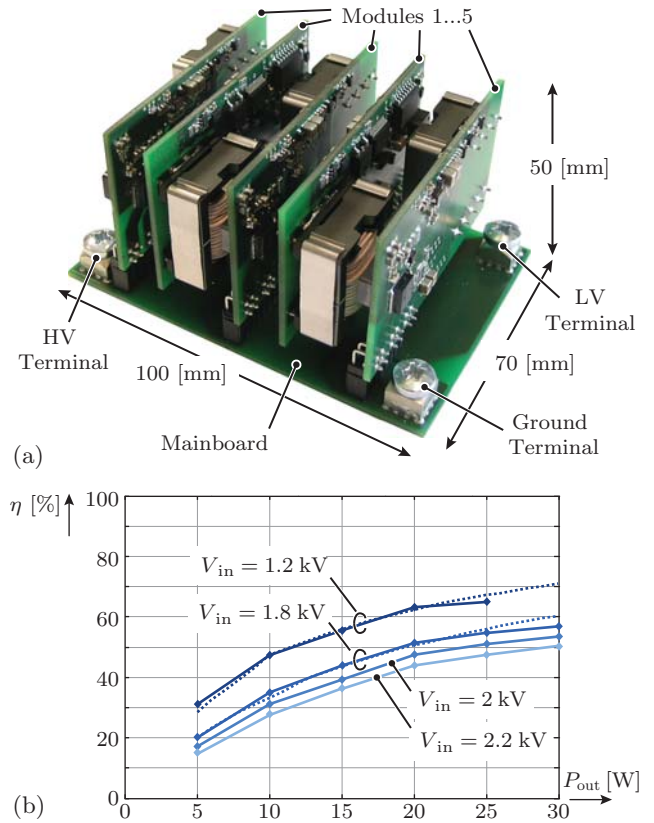


**Fig. 7** (a) Prototype of a modular auxiliary supply for high conversion ratios with  $N_b = 5$  balancing modules operated from a DC-voltage of  $V_{in} = 2$  kV, an output voltage of  $V_{out} = 400$  V, and an output power of  $P_{out} = 30$  W [14]. (b) Efficiency measurement results for different input voltages as a function of the output power.

which has a power rating that is several magnitudes larger than the auxiliary power.

Therefore, in [14] a fully modular “Rainstick” auxiliary power supply is presented with 5 current diverter modules for a voltage conversion from  $V_{in} = 2.4$  kV to  $V_{out} = 400$  V and an output power of  $P_{out} = 30$  W where only semiconductors with a blocking voltage of  $V_{DS,\max} = 1$  kV are employed (cf. **Fig. 7**). The diverter modules also feature on-board auxiliary power supply units with low component count and simple hysteretic control, which allow them to operate completely independently from the other modules. Since the power is not at once directly transferred from the source to the load but through a cascade of different diverter stages, comparable to the pebbles falling down in a rainstick, the converter was named accordingly.

## 5 Advanced Current Diverter Concepts

As mentioned in the previous sections, a disadvantage of the current diverter concept is the influence of the

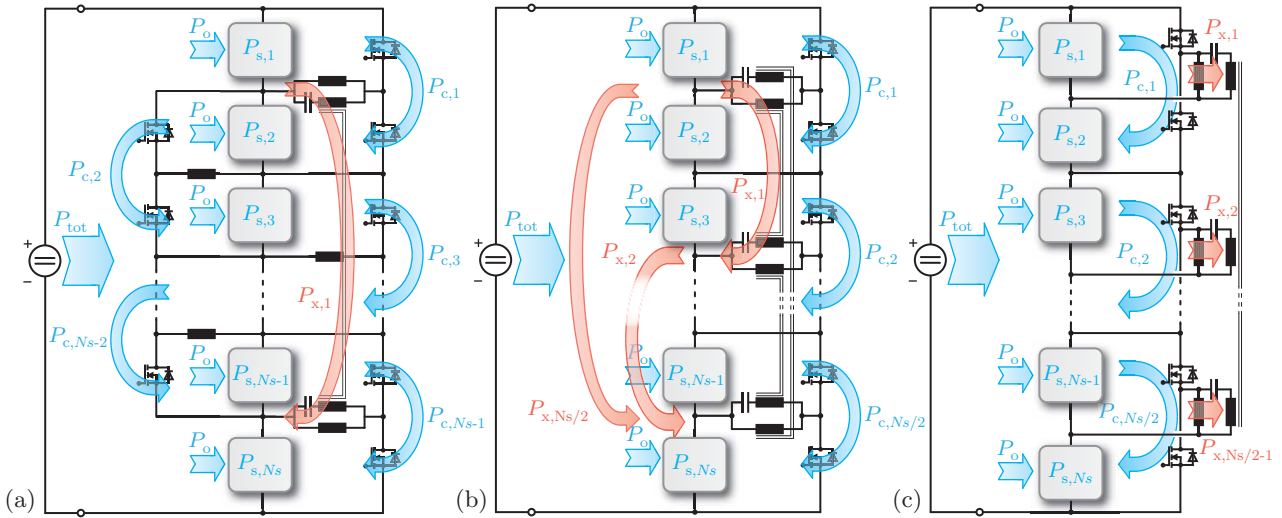


**Fig. 8** Current diverter concepts employing coupled inductors: (a) daisy chain configuration where coupled inductors allow to transfer power from the first diverter module to the last one, and vice versa; (b) use of coupled inductors to reduce the overall component count by reducing the number of required diverter modules; (c) coupling all diverter modules on a common core which enables the direct power transfer between all diverter modules.

number of sources  $N_s$  on the power transfer through the diverter modules. This is especially unfavorable for the application in PV energy systems, but is also a disadvantage for the Rainstick converters, where each diverter module has to be designed for a power rating (almost) equal to the load power. In addition, due to the coupled nature of the power flows between the cells through the converters, a potential defect of a single balancing converter would lead to an interruption of the power flow and thus to unbalanced cell voltage. Depending on the application, this could lead to a failure of the entire system, whereas full-power converter architectures can typically continue to operate (with reduced system power) in the event of a single converter failure. One possibility to mitigate or even remedy the mentioned problems is to couple the inductors of diverter modules.

The first option is to insert/add coupled inductors in the first and last diverter module. Together with series connected capacitors, this creates a series resonant converter (SRC) structure as shown in **Fig. 8(a)**. The resonant frequency of the SRC (defined by the leakage inductance of the coupled inductors and the resonant capacitor) can be tuned to the switching frequency of the diverter modules in order to operate the SRC in half-cycle discontinuous conduction mode (HC-DCM), i.e. as DC transformer with (nearly) load independent ratio of input and output voltage [19]. The SRC allows to transfer power directly between the first and the last module which creates a daisy chain (i.e. ring) structure. As a result, the maximum power which is transferred in any diverter module or the module employing the

coupled inductor is half of the maximum power of the uncoupled structure. This can be intuitively explained, by considering that the power flow can be divided into two paths in the ring structure. The disadvantage of this option, however, is the required voltage isolation of the coupled inductors which has to be rated for the full input voltage.

The second option is to cyclically couple each diverter module with the neighboring diverter modules. With this arrangement, the SRC topology can be used to minimize the component count of the system, as shown in **Fig. 8(b)**. Instead of employing  $N_s - 1$  inductors and  $2 \cdot (N_s - 1)$  switches as in the uncoupled structure, the proposed concept with SRCs employs only  $N_s$  switches and  $N_s/2$  sets of coupled inductors with  $N_s/2$  capacitors for the resonant operation. The SRCs are used to transfer power from two sources to another two sources, e.g. the power  $P_{x,1}$  is transferred from  $P_{s,1}$  to  $P_{s,3}$  and  $P_{s,2}$  to  $P_{s,4}$ , and vice versa. In order to balance the power between  $P_{s,1}$  and  $P_{s,2}$  or  $P_{s,3}$  and  $P_{s,4}$  etc., the magnetizing currents of the SRC converters are used. It should be noted, that the magnetizing current will have a DC-offset if the power levels of the two sources on one side of the SRC are unequal. Thus, the magnetizing current can only balance the sources on the side of an SRC where no resonant capacitor is present. This is also visualized in **Fig. 9**, where the current  $i_p$  can have a DC-offset if the voltages  $V_1$  and  $V_2$  are unequal (i.e. a DC-offset in the magnetizing current is created in order to balance the voltages  $V_1$  and  $V_2$ ), while the resonant capacitor  $C_{res}$  between  $V_3$  and  $V_4$  also functions as a DC-blocking capacitor, which prevents current  $i_s$

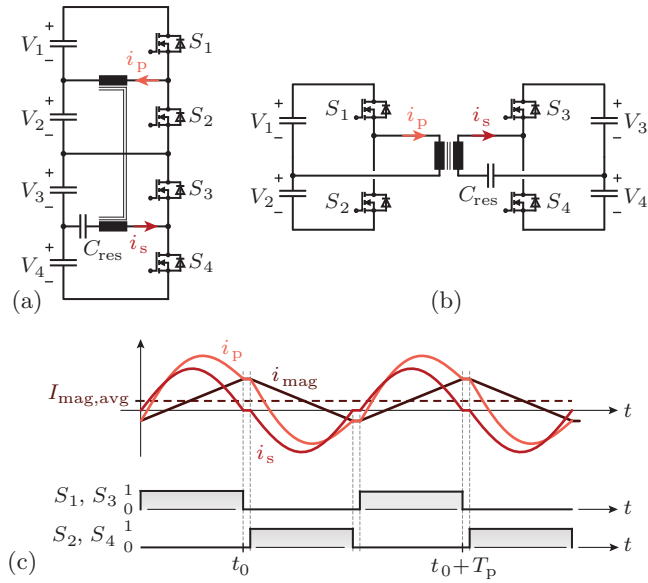


**Fig. 9** Detailed explanation of the operation of diverter modules with coupled inductors: (a) coupled inductors (turn ratio 1 : 1) as proposed for the current diverters. Opening the stack of capacitors in (a) between  $C_2$  and  $C_3$  yields the equivalent series resonant converter (SRC) in (b); (c) characteristic current waveforms and switching patterns of the SRC where the current  $i_p$  is the sum of the current  $i_s$  and the magnetizing current  $i_{mag}$ . Due to the presence of the resonant capacitor  $C_{res}$ , the current of  $i_s$  cannot show any DC-offset, while a DC-offset can result in the current  $i_{mag}$  (and thus also in  $i_p$ ) if the voltages  $V_1$  and  $V_2$  are unequal.

from having a DC-offset. In case the resonant capacitors are placed on both sides of the coupled inductors, additional inductors have to be employed in at least one diverter module, which then allows to balance two neighboring sources.

The third option for further minimizing the power rating of the diverter modules is to assemble all coupled inductors on a common core, as visualized in **Fig. 8(c)**. This does not only reduce the number of coupled inductors to just one multi-terminal coupling device, but also enables the direct power flow between all diverter modules. Each SRC transfers the power level of

$$P_{x,i} = \underbrace{\frac{2}{N_s} \cdot \sum_{j=1}^{N_s} P_{s,j}}_{\text{Twice the avg. of all sources}} - \underbrace{\sum_{j=2i-1}^{2i} P_{s,j}}_{\text{Sources at div. mod. } i} \quad (21)$$

The power transferred via the uncoupled inductors can be calculated as

$$P_{c,i} = \frac{1}{2} (P_{s,2i} - P_{s,(2i-1)}) \quad (22)$$

which is just required to balance the two sources on one side of the SRC modules.

When applying the option of **Fig. 8(c)** to the worst case scenario in PV energy systems (i.e. the PV string is divided into a shaded and an unshaded half) the maximum power level that has to be processed by any SRC equals

$$P_{x,max} = P_{MPP} \cdot (1 - k_{sh}) \quad (23)$$

which is independent of the number of PV modules in the string and is just the power difference between the shaded and the unshaded PV modules which is always lower than the power which would have to be processed by full-power converters [17].

Despite the various advantages, there are also some disadvantages resulting from the employment of coupled inductors. Foremost, the operation of the diverter modules can no longer function without synchronizing the switching patterns between the diverters. This mandates the implementation of some sort of communication or synchronization signal among the diverters which leads to additional hardware and wiring effort. Another drawback especially of the concept with only one common core for coupling all diverters lies in the loss of modularity. The system and particularly the multi-terminal coupled inductor has to be designed for a specific number of sources and can no longer be easily extended for larger numbers of sources as given for the uncoupled system. Finally, in systems with physically distributed sources (e.g. PV modules on a rooftop) it can be difficult to couple all balancing modules on a single core.

## 6 Conclusion

The application of a power flow analysis to string current diverters employed in PV system reveals that for worst case scenarios (which are relevant for the converter dimensioning) the required power ratings of the diverters can exceed the power of the individual PV modules. Consequently, by limiting the power ratings of the diverter modules to only a fraction of the PV module power, a considerable part of the theoretical available power cannot be harvested. In fact, the gain in power output compared to using only bypass diodes is limited and reduces with longer string lengths.

For the “Rainstick” power supply that features high conversion ratios, it is shown with the proposed analysis, that the power rating of the diverter modules approaches the load power level for large numbers of diverters, which reduces the benefits of the partial power conversion concept. However, the advantages of this

concept are the modularity of the system, i.e. scalability and/or adaptability to different conversion ratios, the reduction of voltage stress for the employed semiconductors compared to full-power concepts, and the absence of any communication between the diverter modules due to the operation with fixed duty cycles of 50%. Thus, this concept is especially well suited for high-voltage environments where a high step-down conversion is required for powering low-voltage/power equipment, e.g. as an auxiliary supply.

Moreover, the concept of coupling the inductors of the diverter modules is presented, which allows to reduce the required power rating of the diverter modules and/or to minimize the number of required diverter modules. Furthermore, the coupled inductors also provide additional redundant paths for the power flow which can reduce the impact of a converter failure on the operation of the system.

## References

1. J. W. Kolar, F. Krismer, Y. Lobsiger, J. Muehlethaler, T. Nussbaumer, and J. Miniboeck, "Extreme Efficiency Power Electronics," in *Proc. of the 7th Int. Conf. of Integrated Power Electronics Systems (CIPS)*, pp. 1–22, 2012.
2. Y.-S. Lee and M.-W. Cheng, "Intelligent Control Battery Equalization for Series Connected Lithium-Ion Battery Strings," *IEEE Trans. Ind. Electron.*, vol. 52, no. 5, pp. 1297–1307, 2005.
3. N. H. Kutkut, "A Modular Nondissipative Current Diverter for EV Battery Charge Equalization," in *Proc. of the 13th IEEE Applied Power Electronics Conference (APEC)*, vol. 2, pp. 686–690, 1998.
4. J. McClurg, R. C. N. Pilawa-Podgurski, and P. S. Shenoy, "A Series-Stacked Architecture for High-Efficiency Data Center Power Delivery," in *Proc. of the IEEE Energy Conversion Congress and Exposition (ECCE USA)*, pp. 170–177, Sep. 2014.
5. G. K. Steinke and A. Rufer, "Use of a DC-DC Step Up Converter in Photovoltaic Plants for Increased Electrical Energy Production and Better Utilization of Covered Surface Area," in *Proc. of the Int. Conference on Power Electronics, Intelligent Motion, Renewable Energy and Energy Management (PCIM Europe)*, pp. 1648–1655, May 2015.
6. A. Rufer, "A Five-Level NPC Photovoltaic Inverter with an Actively Balanced Capacitive Voltage Divider," in *Proc. of the Int. Conference on Power Electronics, Intelligent Motion, Renewable Energy and Energy Management (PCIM Europe)*, pp. 172–179, May 2015.
7. A. Rufer, P. Barrade, and G. Steinke, "Voltage Step-Up Converter Based on Multistage Stacked Boost Architecture (MSBA)," in *Proc. of the Int. Power Electronics Conference (IPEC-ECCE Asia)*, pp. 1081–1086, May 2014.
8. P. S. Shenoy and P. T. Krein, "Differential Power Processing for DC Systems," *IEEE Trans. Power Electron.*, vol. 28, no. 4, pp. 1795–1806, 2013.
9. H. J. Bergveld, D. Buethker, C. Castello, T. Doorn, A. de Jong, R. van Otten, and K. de Waal, "Module-Level DC/DC Conversion for Photovoltaic Systems: The Delta-Conversion Concept," *IEEE Trans. Power Electron.*, vol. 28, no. 4, pp. 2005–2013, 2013.
10. S. Qin, C. B. Barth, and R. C. N. Pilawa-Podgurski, "Enhancing Microinverter Energy Capture with Submodule Differential Power Processing," *IEEE Trans. Power Electron.*, vol. 31, no. 5, pp. 3575–3585, 2016.
11. C. Olalla, C. Deline, D. Clement, Y. Levron, M. Rodriguez, and D. Maksimovic, "Performance of Power-Limited Differential Power Processing Architectures in Mismatched PV Systems," *IEEE Trans. Power Electron.*, vol. 30, no. 2, pp. 618–631, 2015.
12. P. S. Shenoy, K. A. Kim, B. B. Johnson, and P. T. Krein, "Differential Power Processing for Increased Energy Production and Reliability of Photovoltaic Systems," *IEEE Trans. Power Electron.*, vol. 28, no. 6, pp. 2968–2979, 2013.
13. J. T. Stauth, M. D. Seeman, and K. Kesarwani, "Resonant Switched-Capacitor Converters for Sub-Module Distributed Photovoltaic Power Management," *IEEE Trans. Power Electron.*, vol. 28, no. 3, pp. 1189–1198, 2013.
14. M. Kasper, D. Bortis, and J. W. Kolar, "Novel High Voltage Conversion Ratio "Rainstick" DC/DC Converters," in *Proc. of the IEEE Energy Conversion Congress and Exposition (ECCE USA)*, pp. 789–796, 2013.
15. M. Kasper, S. Herden, D. Bortis, and J. W. Kolar, "Impact of PV String Shading Conditions on Panel Voltage Equalizing Converters and Optimization of a Single Converter System with Overcurrent Protection," in *Proc. of the 16th European Conference on Power Electronics and Applications (EPE-ECCE Europe)*, pp. 1–10, 2014.
16. K. A. Kim, P. S. Shenoy, and P. T. Krein, "Converter Rating Analysis for Photovoltaic Differential Power Processing Systems," *IEEE Trans. Power Electron.*, vol. 30, no. 4, pp. 1987–1997, Apr. 2015.
17. M. Kasper, D. Bortis, and J. W. Kolar, "Classification and Comparative Evaluation of PV Panel-Integrated DC-DC Converter Concepts," *IEEE Trans. Power Electron.*, vol. 29, no. 5, pp. 2511–2526, 2014.
18. G. R. Walker and J. C. Pierce, "Photovoltaic DC-DC Module Integrated Converter for Novel Cascaded and Bypass Grid Connection Topologies — Design and Optimisation," in *Proc. of the 37th IEEE Power Electronics Specialists Conf. (PESC)*, pp. 1–7, 2006.
19. J. Huber, G. Ortiz, F. Krismer, N. Widmer, and J. W. Kolar, " $\eta$ - $\rho$  Pareto Optimization of Bidirectional Half-Cycle Discontinuous-Conduction-Mode Series-Resonant DC/DC Converter with Fixed Voltage Transfer Ratio," in *Proc. of the 28th IEEE Applied Power Electronics Conference and Exposition (APEC)*, pp. 1413–1420, 2013.